J. Am. Chem. Soc. 1988, 110, 823-830

Nonanuclear Oxide-Bridged Manganese Complex. Preparation, Structure, and Magnetic Properties of $[Mn_9O_4(O_2CPh)_8(sal)_4(salH)_2(pyr)_4]$ ($salH_2$ = Salicylic Acid; pyr = Pyridine)

Cheryl Christmas,[1a] John B. Vincent,[1a] Hsiu-Rong Chang,[1b] John C. Huffman,[1c] George Christou,*[1a,d] and David N. Hendrickson*[1b]

Contribution from the Department of Chemistry and Molecular Structure Center, Indiana University, Bloomington, Indiana 47405, and School of Chemical Science, University of Illinois, Urbana, Illinois 61801. *Received July 3, 1987*

Abstract: The preparation of a mixed-valence nonanuclear manganese complex with mixed salicylate/benzoate/pyridine ligation is described. Treatment of $[Mn_3O(O_2CPh)_6(pyr)_2(H_2O)]$ with 3 equiv of salicylic acid ($salH_2$) in CH_3CN leads to the formation of $[Mn_9O_4(O_2CPh)_8(sal)_4(salH)_2(pyr)_4]$ (**5**), where pyr is pyridine. Complex **5** crystallizes in the monoclinic space group $C2/c$ with, at −155 °C, $a = 17.625$ (13) Å, $b = 38.314$ (35) Å, $c = 19.886$ (16) Å, $\beta = 99.17$ (4)°, and $Z = 4$. The structure was solved and refined with a total of 3168 unique reflections with $F > 2.33\sigma(F)$. Final values of conventional discrepancy indices R and R_w are 9.70 and 9.92%, respectively. The structure consists of two butterfly-like $[Mn_4(\mu_3\text{-}O)_2]$ units, containing octahedral Mn^{III} ions, linked together by a bridging $Mn(sal)_4$ central unit. The latter contains an eight-coordinate Mn^{II} ion and is the site of a crystallographic C_2 axis relating the halves of the molecule. The sal^{2-} groups linking the Mn^{II} and $[Mn_4O_2]$ units have a rare μ_3-η^3-bridging mode; peripheral ligation to the complete molecule is provided by eight μ_2-$PhCOO^-$, four terminal pyr, and two μ_2-$salH^-$ groups, employing only their carboxylate functions with the phenoxide oxygen atoms protonated and not bound to a manganese ion. The complex possesses an average metal oxidation state of +2.89 and is a rare example of a discrete high-nuclearity manganese species. The results of solid-state magnetic susceptibility studies in the temperature range 300.9–5.0 K are described. The effective magnetic moment per molecule (μ_{eff}) gradually decreases from a value of 11.82 μ_B at 300.9 K to a value of 5.83 μ_B at 5.0 K. The derivation of a theoretical model to account for the intramolecular magnetic exchange interactions in **5** by the Kambe vector coupling approach is described. Least-squares fitting of the susceptibility data to the model gives exchange parameters for the butterfly-like $[Mn_4(\mu_3\text{-}O)_2]$ units of $J = -26.2$ cm^{-1} for the $(\mu\text{-}O)_2Mn^{III}$ interaction, $J = -11.2$ cm^{-1} for the "hinge"–"wing-tip" $(\mu\text{-}O)_2Mn^{III}{}_2$ interaction, and $J = -0.97$ cm^{-1} for the eight $Mn^{II}\cdots Mn^{III}$ interactions. Of the 209 725 states of **5**, the ground state is found to be a $S = {}^3/_2$ state, with more than 3000 states found within 150 cm^{-1} of the ground state.

The most important biological role identified to date for the metal manganese is the enzyme responsible for water oxidation/oxygen evolution in the photosynthetic apparatus of higher plants and cyanobacteria.[2-5] It is now generally believed that a tetranuclear manganese aggregate represents the site of water oxidation on the donor side of photosystem II (PS II), and much effort continues to be expended on elucidating the structure and mode of action of this unit during the catalytic cycle. The manganese complex is capable of cycling between five distinct oxidation levels (the S_n states,[6] n = 0–4), and it is widely accepted that these involve the higher oxidation states (II–IV) of the metal.[4,7] A superreduced level labeled S_{-1} is also accessible under certain conditions.[8]

Syntheses of inorganic models of the various S_n states are a current goal, and in recent reports, we have described how reaction of the trinuclear complexes $[Mn_3O(O_2CR)_6L_3]^Z$ (R = H, Me, Et, Ph; L = pyridine (pyr), H_2O; Z = 0, 1) with 2,2′-bipyridine (bpy) leads to the assembly of tetranuclear $[Mn_4O_2(O_2CMe)_6(bpy)_2]$ (**1**) and $[Mn_4O_2(O_2CR)_7(bpy)_2]^{Z+}$ (**2**, Z = 0, R = Ph; **3**, Z = 1, R = Me), with structural features and average oxidation levels (+2.5, +2.75, +3.0, respectively) bearing close correspondence to those deduced for the native site.[9,10] We have therefore proposed complexes **1**–**3** as potential models for the S_{-1}, S_0, and S_1 states, respectively. More recently, we described the synthesis of the complex $[Mn_4O_3Cl_6(O_2CMe)_3(HIm)]^{2-}$ (**4**, HIm = imidazole), with structural features and oxidation level (+3.25) corresponding to the S_2 state.[11]

Since tyrosine phenoxide ligation to the Mn_4 aggregate in the enzyme is a possibility, we have sought to extend the above work by incorporating this ligand type into our synthetic materials. Initial work showed monodentate phenols to be oxidized by the manganese centers. Attention was turned then to the mixed carboxylate/phenoxide ligand salicylic acid ($salH_2$), which is resistant to oxidation by Mn^{3+}. Herein are described the results of this investigation, the synthesis, and magnetochemistry of the remarkable mixed-valence nonanuclear complex $[Mn_9O_4(O_2CPh)_8(sal)_4(salH)_2(pyr)_4]$ (**5**).

High-nuclearity oxo-bridged metal complexes are of interest for a number of reasons. There is growing attention paid to the preparation of models for the core of the iron-storage protein ferritin.[12] An octanuclear Fe^{III} complex containing 1,4,7-tria-

---

[1] (a) Department of Chemistry, Indiana University. (b) University of Illinois. (c) Molecular Structure Center, Indiana University. (d) Alfred P. Sloan Research Fellow, 1987–1989.

[2] Asmez, J. *Biochim. Biophys. Acta* **1983**, *726*, 1.

[3] Dismukes, G. C. *Photochem. Photobiol.* **1986**, *43*, 99.

[4] (a) Goodin, D. B.; Yachandra, V. K.; Britt, R. D.; Sauer, K.; Klein, M. P. *Biochim. Biophys. Acta* **1984**, *767*, 209. (b) Yachandra, V. K.; Guiles, R. D.; McDermott, A.; Britt, R. D.; Dexheimer, S. L.; Sauer, K.; Klein, M. P. *Biochim. Biophys. Acta* **1986**, *850*, 324.

[5] Kuwabara, T.; Miyao, M.; Murata, N. *Biochim. Biophys. Acta* **1985**, *806*, 283.

[6] Kok, B.; Forbush, B.; McGloin, M. *Photochem. Photobiol.* **1970**, *11*, 457.

[7] Srinivasan, A. N.; Sharp, R. R. *Biochim. Biophys. Acta* **1986**, *850*, 211.

[8] (a) Velthuys, B.; Kok, B. *Biochim. Biophys. Acta* **1978**, *502*, 211. (b) Schmid, G. H.; Thibault, P. *Z. Naturforsch. C: Biosci.* **1983**, *38C*, 60. (c) Bader, K. P.; Thibault, P.; Schmid, G. H. *Z. Naturforsch., C: Biosci.* **1983**, *38C*, 778. (d) Pistorius, E. K.; Schmid, G. H. *Biochim. Biophys. Acta* **1987**, *890*, 352.

[9] Vincent, J. B.; Christmas, C.; Huffman, J. C.; Christou, G.; Chang, H.-R.; Hendrickson, D. N. *J. Chem. Soc., Chem. Commun.* **1987**, 236.

[10] Christmas, C.; Vincent, J. B.; Huffman, J. C.; Christou, G.; Chang, H.-R.; Hendrickson, D. N. *J. Chem. Soc., Chem. Commun.* **1987**, 1303.

[11] Bashkin, J. S.; Chang, H.-R.; Streib, W. E.; Huffman, J. C.; Hendrickson, D. N.; Christou, G. *J. Am. Chem. Soc.* **1987**, *109*, 6502–6504.

[12] (a) Ford, G. C.; Harrison, P. M.; Rice, D. W.; Smith, J. M. A.; Treffry, A.; White, J. L.; Yariv, J. *Rev. Port. Quim.* **1985**, *27*, 119. (b) Ford, G. C.; Harrison, P. M.; Rice, D. W.; Smith, J. M. A.; Treffry, A.; White, J. L.; Yariv, J. *Philos. Trans. R. Soc. London, B* **1984**, *304*, 551–565. (c) Spiro, T. G.; Saltman, P. *Struct. Bonding (Berlin)* **1969**, *6*, 116–156. (d) Theil, E. C. *Adv. Inorg. Biochem.* **1983**, *5*, 1–38.

0002-7863/88/1510-0823$01.50/0 © 1988 American Chemical Society

zacyclononane (TACN) nonbridging ligands, $[Fe_8O_2(OH)_{12}(TACN)_6]^{8+}$, has been reported.[13] Several planar tetranuclear cores of the type $[Fe_4(\mu_3\text{-}O)_2]^{8+}$ or $[Fe_4(\mu_3\text{-}OH)_2]^{10+}$ have been encountered in nature.[14,15] Murch et al.[16] recently reported a tetrahedral $[Fe_4(\mu_2\text{-}O)_2(\mu_2\text{-}OH)_2(\mu_2\text{-}OR)_2]^{4+}$ species. Very recently Gorun et al.[17] reported the structure and detailed characterization of a novel discrete undecairon(III) oxo–hydroxo aggregate $[Fe_{11}O_6(OH)_6(O_2CPh)_{15}]$. Controlled hydrolytic polymerization in nonaqueous solvents of simple mononuclear and oxo-bridged binuclear ferric salts was employed to prepare this $Fe^{III}{}_{11}$ complex. However, there still is not a systematic synthetic approach available to prepare larger and larger oxo-bridged complexes. The parallelism between the chemistries of iron and manganese with oxygen and nitrogen ligands indicates that strategies developed for preparing high-nuclearity manganese complexes could be applicable to preparing ferritin models.

Fundamental information about single-domain magnetic oxides could also be forthcoming from the characterization of discrete high-nuclearity oxo-bridged metal complexes. Single-domain particles of magnetite, Fe_3O_4, behave as paramagnets when their diameters are less than ~20 Å.[18] Magnetite particles with diameters in the range of ~20–300 Å exhibit superparamagnetism. Not only ferromagnets such as magnetite or doped magnetites (e.g., $MnFe_2O_4$) but also classical antiferromagnets such as NiO and Cr_2O_3 have been shown to exhibit superparamagnetism.[18,19] In paramagnets the magnetic moments of the metal ions act independently of each other. In a superparamagnet all of the individual magnetic moments in the single domain particles are aligned parallel (or antiparallel) as a result of the interion magnetic exchange interactions. Furthermore, the net magnetization of a superparamagnet is rapidly changing direction as a result of thermal fluctuations. Magnetite particles with diameters larger than ~300–400 Å have a greater magnetic exchange interaction than that for superparamagnetic particles and, as a result, hysteresis and permanent magnetization. These phenomena have only been studied with distributions of particle sizes. Access to a series of well-characterized high-nuclearity oxide-bridged metal complexes would lead to a better understanding of the paramagnet/superparamagnet/ferromagnet interfaces.

Experimental Section

Synthesis. All operations were carried out under aerobic conditions at ambient temperature. All solvents and salicylic acid were used as received. The complex $[Mn_3O(O_2CPh)_6(pyr)_2(H_2O)]\cdot 0.5CH_3CN$ was available from previous work.[20]

To a stirred green-brown solution of $[Mn_3O(O_2CPh)_6(pyr)_2(H_2O)]\cdot 0.5CH_3CN$ (1.10 g, 1.00 mmol) in CH_3CN (30 mL) was added solid salicylic acid (0.41 g, 3.00 mmol). The acid soon dissolved, and the homogeneous dark brown solution was allowed to stand undisturbed at ambient temperature overnight. The resulting black crystals of $[Mn_9O_4(O_2CPh)_8(sal)_4(salH)_2(pyr)_4]$ were collected by filtration, washed with hexanes, and dried in vacuo. Yields are typically in the 35–40% range. Recrystallization from CH_2Cl_2/hexanes gave well-formed black needles. Anal. Calcd for $C_{118}H_{86}N_4O_{38}Mn_9$: C, 53.23; H, 3.26; N, 2.10; Mn, 18.57. Found: C, 53.07; H, 3.53; N, 2.05; Mn, 17.9. The analysis sample was dried in vacuo; the sample for crystallography was not dried as it undergoes solvent loss and loss of crystallinity. Electronic spectrum (CH_2Cl_2) [λ_{max}, nm (ϵ_M/Mn^{III}, L mol^{-1} cm^{-1})]: 250 (1.6×10^4), 299 (6.5×10^3), 508 (507), 722 (191).

Table I. Crystallographic Data

parameter	value
formula	$C_{118}H_{86}N_4O_{38}Mn_9$
M_r	2662.47
cryst syst	monoclinic
space group	$C2/c$
temp, °C	−155
a, Å	17.625 (13)[a]
b, Å	38.314 (35)
c, Å	19.886 (16)
β, deg	99.17 (4)
V, Å^3	13 256.64
Z	4
cryst dimens, mm	$0.20 \times 0.25 \times 0.40$
Mo Kα radiatn: λ, Å	0.710 69[b]
abs coeff, cm^{-1}	8.660
scan speed, deg/min	4.0 ($\theta/2\theta$)
scan width, deg	2.0 + dispersion
data collcd	$6° \leq 2\theta \leq 45°$
total no. of data	8119
no. of unique data	6164
averaging R[c]	0.085
obsd data, $F > 2.33\sigma(F)$	3168
R, %	9.70[d]
R_w, %	9.92[e]
goodness of fit	1.754[f]

[a] 36 reflections at −155 °C. [b] Graphite monochromator. [c] 1665 reflections measured more than once. [d] $R = \sum||F_o| - |F_c||/\sum|F_o|$. [e] $R_w = [\sum w(|F_o| - |F_c|)^2/\sum w|F_o|^2]^{1/2}$ where $w = 1/\sigma^2(|F_o|)$. [f] Goodness of fit $= [\sum w(|F_o| - |F_c|)^2/(N_{obsn} - N_{para})]^{1/2}$.

X-ray Crystallography. Data were collected at approximately −155 °C on a Picker four-circle diffractometer; full details of the diffractometry, low-temperature facilities, and computational procedures employed by the Molecular Structure Center are available elsewhere.[21] Data collection parameters are summarized in Table I. A systematic search of a limited hemisphere of reciprocal space located a set of diffraction maxima with symmetry and systematic absences consistent with the two space groups $C2/c$ and Cc. Subsequent solution and refinement of the structure confirmed the centrosymmetric choice $C2/c$. The structure was solved by the usual combination of direct methods (MULTAN) and Fourier techniques and refined by full-matrix least squares. The molecule lies on a crystallographic C_2 axis. Even so, the resulting large number of independent atoms necessitated refinement of only manganese atoms with anisotropic thermal parameters; all other atoms were refined with isotropic parameters. No attempt to find or include hydrogen atoms was made. In the latter stages, a difference Fourier revealed the presence of peaks assignable to seriously disordered CH_2Cl_2 molecules with partial occupancy. The three largest peaks and several smaller ones were included in the final refinement cycles as Cl and C atoms, respectively. A final difference Fourier was essentially featureless, with the largest peak being 0.43 e/Å^3.

Physical Measurements. Variable-temperature, solid-state magnetic susceptibility data were measured with a Series 800 VTS-50 SQUID susceptometer (SHE Corp.) maintained by the Physics Department at the University of Illinois. The susceptometer was operated at a magnetic field strength of 10 kG. Diamagnetic corrections were estimated from Pascal's constants (-1267×10^{-6} cgsu for complex **5**) and subtracted from the experimental susceptibility data to obtain the molar paramagnetic susceptibility of the compound.

Results and Discussion

Synthesis. The stimulus for this work stemmed from the prior observation that bipyridine (bpy) mediates the conversion of trinuclear $[Mn_3O]$ species into tetranuclear $[Mn_4O_2]$ products,[9,10] and we hoped to obtain similar species with salicylate for reasons outlined in the introduction. Treatment of $[Mn_3O(O_2CPh)_6(pyr)_2(H_2O)]$ with 3 equiv of salicylic acid in CH_3CN solution led to a clean reaction from which well-formed black crystals of complex **5** could be obtained in reasonable yield. Further crops can be obtained by addition of hexanes to the reaction filtrate, but we do not routinely perform this to avoid contamination by

---

(13) Wieghardt, K.; Pohl, K.; Jibril, I.; Huttner, G. *Angew. Chem., Int. Ed. Engl.* **1984**, *23*, 77–78.

(14) (a) Susse, P. *Z. Kristallogr.* **1968**, *127*, 261–275. (b) Ponomarev, V. I.; Atovmyan, L. O.; Bobkova, S. A.; Turtě, K. I. *Dokl. Akad. Nauk. SSSR* **1984**, *274*, 368–372.

(15) Moore, P. B. *Ann. Mineral* **1982**, *57*, 397–410.

(16) Murch, B. P.; Boyle, P. D.; Que, L. *J. Am. Chem. Soc.* **1985**, *107*, 6728–6729.

(17) (a) Gorun, S. M.; Papaefthymiou, G. C.; Frankel, R. B.; Lippard, S. J. *J. Am. Chem. Soc.* **1987**, *109*, 3337–3348. (b) Gorun, S. M.; Lippard, S. J. *Nature (London)* **1986**, *319*, 666.

(18) Bate, G. In *Magnetic Oxides*; Craik, D. J., Ed.; Wiley-Interscience: New York, 1975; Part 2, Chapter 12.

(19) Cohen, J.; Creer, K. M.; Pauthenet, R.; Srivastava, K. *J. Phys. Soc. Jpn.* **1962**, *17*, *B1*, 685.

(20) Vincent, J. B.; Chang, H.-R.; Folting, K.; Huffman, J. C.; Christou, G.; Hendrickson, D. N. *J. Am. Chem. Soc.* **1987**, *109*, 5703–5711.

(21) Chisholm, M. H.; Folting, K.; Huffman, J. C.; Kirkpatrick, C. C. *Inorg. Chem.* **1984**, *23*, 1021.

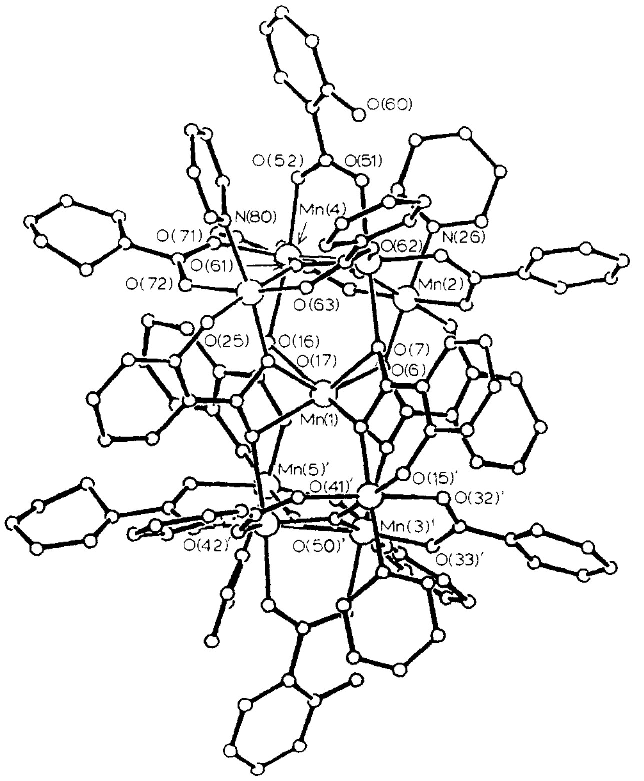

Figure 1. Structure of complex **5**. To avoid congestion, only one of each symmetry-related pair of Mn, O, and N atoms is labeled. Carbon atoms were numbered consecutively from the heteroatoms around aromatic rings.

byproducts or excess reagents. Subsequent crystallographic identification of **5** established that our objective had been both successful and unsuccessful: successful in the sense that salicylate had indeed mediated formation of $[Mn_4O_2]$ units but unsuccessful in that the product was not a discrete tetranuclear species but instead a nonanuclear complex containing *two* Mn_4O_2 units "bridged" by an additional manganese center (vide infra). Charge considerations necessitate a mixed-valence description for **5** (8 Mn^{III}, Mn^{II}), yielding an average metal oxidation state of +2.89. The average metal oxidation state in the trinuclear reagent is +2.67, requiring either the intermediacy of an oxidizing agent, most probably atmospheric O_2, or the formation of a lower oxidation state byproduct, for example a Mn^{II} species. It should also be added, however, that the corresponding reaction with $[Mn_3O(O_2CPh)_6(pyr)_3](ClO_4)$ (average oxidation state +3.0) also yields **5** in comparable yield, the Mn^{II} ion presumably resulting from disproportionation of Mn^{III}. Consequently, we refrain from attempting to rationalize with a balanced equation what is obviously a complex reaction system; suffice it to say that complex **5** must be the thermodynamically governed product of these reaction mixtures.

Description of Structure. Fractional atomic coordinates are listed in Table II; selected bond lengths and angles are listed in Table III. A labeled structure and a stereoview are depicted in Figures 1 and 2, respectively. The disordered CH_2Cl_2 molecules are well separated from the manganese complex and will not be discussed further. The complete molecule lies on an imposed C_2 axis passing through central Mn(1). The molecule possesses no other symmetry elements and belongs to the C_2 point group. The overall structure will be described in two stages: (i) the central Mn(1) and (ii) the "terminal" Mn_4 units.

Central Mn(1) is eight-coordinate, being bound to eight oxygen atoms from four salicylate carboxylate functions. The disposition of the oxygen atoms does not correspond to any idealized eight-coordinate geometry but is adequately described as distorted dodecahedral. Mn(1) is assigned as the unique Mn^{II} center, and Mn(1)–O bond distances (av 2.312 Å) are similar to those in the square-antiprismatic geometry of the 12-crown-4 coordinated cation in $[Mn(C_8H_{16}O_4)_2](Br_3)_2$[22a] (av 2.31 Å) and in the dodecahedral eight-coordinate Mn^{II} complex $[Mn(NO_3)_4]^{2-}$ (av 2.306 Å).[22b] The four sal^{2-} groups binding Mn(1) are each also linked to two other manganese atoms, one at the top and one at the bottom of the molecule; each carboxylate oxygen atom is μ_2 while the phenoxide oxygen atoms bind in a terminal fashion. Each ligand is thus a μ_3-η^3-sal^{2-} group, and for clarity, this is depicted.

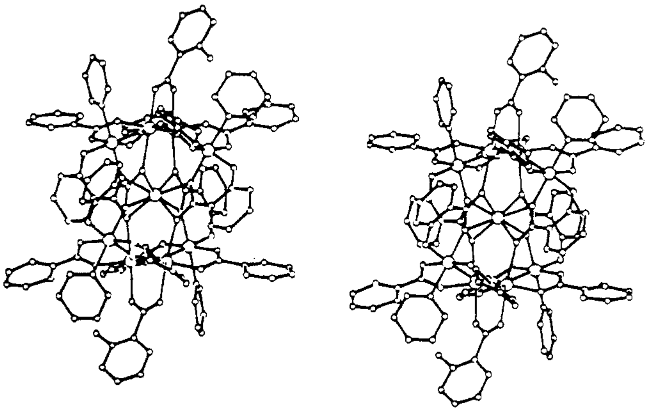

Figure 2. Stereoview of complex **5**. The view is approximately (but, for clarity, not exactly) down the imposed C_2 axis.

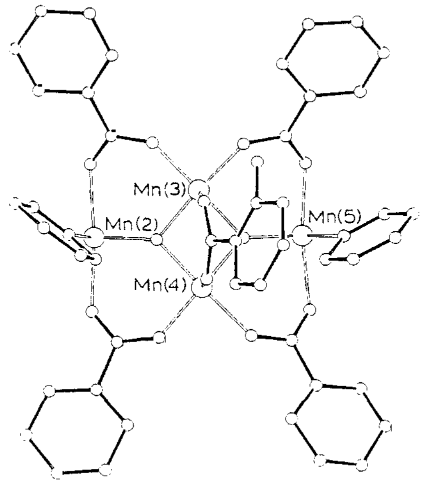

Figure 3. Top view of a portion of complex **5** clarifying the structure of the $[Mn_4(\mu_3\text{-}O)_2]$ unit.

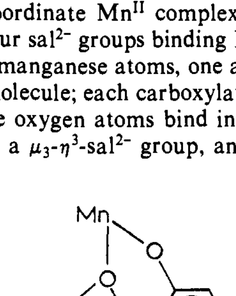

This mode of binding for salicylate is extremely rare and was seen previously, to our knowledge, only in lanthanide and actinide chemistry, specifically for one of the three sal^{2-} ligands in structurally characterized $M(sal)_3(H_2O)$ (M = Am, Sm)[23] and for the M = La and Nd complexes, which are isomorphous.

The remaining eight Mn^{III} atoms are disposed in two $[Mn_4(\mu_3\text{-}O)_2]$ units. These units have the same butterfly arrangement as found in the discrete $[Mn_4O_2(OAc)_7(bpy)_2]^+$ complex (**3**),[9] and the precise structure of one unit is shown in Figure 3. The μ_3-oxide atoms O(41) and O(61) are slightly above their respective

---

(22) (a) Hughes, B. B.; Haltiwanger, R. C.; Pierpont, C. G.; Hampton, M.; Blackmer, G. L. *Inorg. Chem.* **1980**, *19*, 1801. (b) Drummond, J.; Wood, J. S. *J. Chem. Soc. A* **1970**, 226.

(23) Burns, J. H.; Baldwin, W. H. *Inorg. Chem.* **1977**, *16*, 289.

Table II. Fractional Coordinates (×10^4) and Thermal Parameters (×10)[a]

atom	x	y	z	B_{iso}
Mn(1)	5000*	1522 (1)	7500*	22
Mn(2)	3108 (2)	1964 (1)	6656 (2)	25
Mn(3)	3284 (2)	1809 (1)	8361 (2)	22
Mn(4)	2959 (2)	1206 (1)	7556 (2)	26
Mn(5)	4190 (2)	1077 (1)	9051 (2)	26
O(6)	4213 (8)	1849 (4)	6758 (7)	26 (3)
O(7)	4568 (8)	1924 (4)	8273 (7)	23 (3)
C(8)	4762 (13)	2023 (6)	6495 (12)	26 (5)
C(9)	4575 (12)	2303 (6)	6020 (11)	21 (5)
C(10)	5170 (12)	2493 (6)	5796 (11)	25 (5)
C(11)	5036 (13)	2770 (6)	5361 (12)	27 (5)
C(12)	4253 (13)	2882 (6)	5093 (12)	29 (5)
C(13)	3658 (12)	2694 (6)	5334 (11)	24 (5)
C(14)	3799 (13)	2409 (6)	5759 (12)	28 (5)
O(15)	3171 (8)	2233 (4)	5913 (8)	30 (3)
O(16)	4115 (7)	1086 (4)	7123 (7)	23 (3)
O(17)	4972 (7)	1195 (4)	8465 (7)	22 (3)
O(18)	4425 (12)	888 (6)	6627 (11)	22 (5)
C(19)	4212 (12)	707 (6)	6200 (11)	22 (5)
C(20)	3659 (13)	467 (6)	6365 (12)	27 (5)
C(21)	3412 (13)	174 (6)	5964 (12)	30 (5)
C(22)	6252 (14)	114 (7)	9674 (13)	40 (6)
C(23)	5677 (13)	348 (6)	9834 (12)	29 (5)
C(24)	5474 (12)	633 (6)	9418 (11)	22 (5)
O(25)	4940 (8)	848 (4)	9620 (8)	32 (3)
N(26)	1918 (10)	2107 (5)	6583 (9)	25 (4)
C(27)	1720 (14)	2432 (7)	6426 (12)	34 (6)
C(28)	900 (16)	2539 (7)	6389 (15)	51 (7)
C(29)	420 (15)	2278 (7)	6595 (14)	43 (6)
C(30)	642 (14)	1947 (7)	6755 (13)	39 (6)
C(31)	1446 (14)	1848 (6)	6761 (12)	33 (5)
O(32)	3399 (8)	2430 (4)	7245 (8)	27 (3)
O(33)	3087 (8)	2305 (4)	8271 (7)	23 (3)
C(34)	3212 (12)	2518 (6)	7803 (12)	26 (5)
C(35)	3125 (12)	2889 (6)	7940 (11)	21 (5)
C(36)	3083 (12)	3021 (6)	8595 (11)	24 (5)
C(37)	2996 (13)	3383 (7)	8739 (13)	37 (6)
C(38)	2910 (16)	3611 (8)	8180 (16)	57 (7)
C(39)	2912 (16)	3485 (8)	7500 (16)	56 (7)
C(40)	3061 (14)	3117 (7)	7365 (13)	41 (6)
O(41)	2745 (8)	1527 (4)	6012 (8)	36 (4)
O(42)	2427 (8)	1094 (4)	6663 (7)	27 (3)
C(43)	2463 (13)	1240 (6)	6090 (12)	29 (5)
C(44)	2084 (13)	1039 (6)	5456 (12)	28 (5)
C(45)	1986 (16)	1233 (8)	4876 (16)	54 (7)
C(46)	1607 (19)	1063 (9)	4251 (18)	74 (9)
C(47)	1431 (17)	702 (9)	4308 (17)	64 (8)
C(48)	1536 (16)	515 (8)	4921 (16)	54 (7)
C(49)	1847 (14)	691 (7)	5556 (13)	42 (6)
O(50)	3052 (7)	1690 (3)	7425 (7)	22 (3)
O(51)	2091 (8)	1732 (4)	8526 (7)	24 (3)
O(52)	1845 (8)	1252 (4)	7885 (8)	28 (3)
C(53)	1718 (12)	1466 (6)	8322 (11)	21 (5)
C(54)	1061 (12)	1372 (6)	8731 (12)	24 (5)
C(55)	507 (14)	1116 (7)	8436 (13)	42 (6)
C(56)	−67 (15)	1013 (7)	8828 (14)	49 (7)
C(57)	−58 (13)	1159 (6)	9475 (12)	32 (5)
C(58)	479 (14)	1409 (7)	9765 (13)	39 (6)
C(59)	1036 (13)	1513 (6)	9345 (12)	32 (5)
O(60)	1528 (12)	1761 (5)	9650 (11)	20 (5)
O(61)	3455 (8)	1326 (4)	8438 (7)	29 (3)
O(62)	3484 (8)	1904 (4)	9314 (7)	25 (3)
O(63)	4346 (8)	1508 (4)	9738 (7)	30 (3)
C(64)	3939 (13)	1766 (6)	9820 (12)	29 (5)
C(65)	3894 (12)	1911 (6)	10498 (11)	22 (5)
C(66)	3526 (13)	2234 (6)	10531 (12)	30 (5)
C(67)	3515 (13)	2372 (6)	11220 (13)	37 (6)
C(68)	3793 (17)	2176 (8)	11787 (16)	59 (8)
C(69)	4163 (15)	1865 (7)	11752 (14)	47 (6)
C(70)	4236 (14)	1721 (7)	11086 (14)	43 (6)
O(71)	2889 (8)	706 (4)	7733 (8)	32 (3)
O(72)	3909 (9)	596 (4)	8509 (8)	34 (4)
C(73)	3341 (14)	498 (7)	8105 (13)	36 (6)
C(74)	3107 (19)	121 (8)	8029 (17)	64 (8)
C(75)	3751 (40)	−102 (19)	8424 (36)	191 (24)
C(76)	3358 (68)	−434 (31)	8446 (59)	332 (49)
C(77)	2831 (33)	−564 (14)	7892 (29)	141 (16)
C(78)	2309 (22)	−350 (11)	7522 (20)	89 (10)
C(79)	2489 (16)	24 (8)	7530 (15)	53 (7)
N(80)	3363 (11)	908 (5)	9699 (10)	34 (4)
C(81)	3603 (14)	865 (6)	10352 (13)	37 (6)
C(82)	3098 (14)	754 (6)	10793 (13)	38 (6)
C(83)	2305 (14)	695 (6)	10491 (13)	38 (6)
C(84)	2065 (13)	745 (6)	9823 (13)	37 (6)
C(85)	2622 (13)	853 (6)	9390 (12)	28 (5)

[a] Parameters marked with an asterisk were not varied.

Mn_3 planes as found in **3**. A μ_2-benzoate group bridges each exterior Mn–Mn edge, and each "wing-tip" manganese atom possesses a terminal pyridine ligand. The two "hinge" metals, Mn(3) and Mn(4), are bridged by a μ_2-salH$^-$ ligand, employing only its carboxylate function. Although the data were not of sufficient quality to locate H atoms, phenoxide oxygen O(60) must be protonated and hydrogen-bonded to O(51), a conclusion supported by the O(60)···O(51) separation (2.59 (2) Å), which is similar to those in dinuclear rhodium(II)[24] and molybdenum(II)[25] μ-salH$^-$ complexes (2.49–2.60 (2) Å), and the resulting near-coplanarity between the aromatic ring and the O(51)–C(53)–O(52) plane. The four metal centers are six-coordinate and possess distorted octahedral geometry, with the remaining coordination sites occupied by terminal phenoxide and bridging carboxylate oxygen atoms from the central sal^{2-} groups (not shown in Figure 3). The existence of Mn_4O_2 units with phenoxide–oxygen ligation is thus established, and although the overall nuclearity of **5** is not what might have been anticipated, it augurs well for the possibility of obtaining discrete salicylate-bound complexes, this possibility is currently under further investigation.

It is interesting that complex **5** is a discrete molecular species, given that its numerous oxygen-containing ligands could easily have been expected to provide interunit linkages to form an extended structure as found, for example, in M(sal)$_3$(H$_2$O) (M = Am, Sm)[23] and, more related to this work, in [Mn(EtOH)$_4$][Mn$_2$(sal)$_4$(pyr)$_2$].[26] There are indeed very few examples of discrete high-nuclearity complexes in manganese or related iron chemistry with such ligands and at these higher oxidation levels

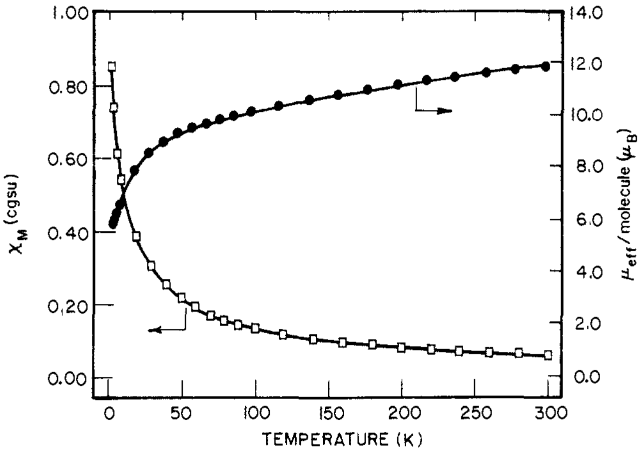

Figure 4. Plots of the molar paramagnetic susceptibility per complex, χ_M, versus temperature and of the effective magnetic moment per complex, μ_{eff}, versus temperature for complex **5**. The solid lines represent the least-squares fit of the magnetic susceptibility data to the theoretical model described in the text.

---

(24) Bancroft, D. P.; Cotton, F. A.; Han, S. *Inorg. Chem.* **1984**, *23*, 2408.
(25) Cotton, F. A.; Mott, G. N. *Inorg. Chim. Acta* **1983**, *70*, 159.
(26) Vincent, J. B.; Folting, K.; Huffman, J. C.; Christou, G. *Inorg. Chem.* **1986**, *25*, 996.

Table III. Selected Bond Lengths (Å) and Angles (deg)

	Bonds		
Mn(1)–O(6)	2.240 (14)	Mn(4)–O(16)	2.381 (14)
Mn(1)–O(7)	2.385 (14)	Mn(4)–O(42)	1.921 (15)
Mn(1)–O(16)	2.325 (14)	Mn(4)–O(50)	1.881 (14)
Mn(1)–O(17)	2.298 (14)	Mn(4)–O(52)	2.173 (15)
		Mn(4)–O(61)	1.887 (15)
Mn(2)–O(6)	1.976 (14)	Mn(4)–O(62)	1.958 (16)
Mn(2)–O(15)	1.819 (16)		
Mn(2)–O(32)	2.150 (15)	Mn(5)–O(17)	1.994 (14)
Mn(2)–O(41)	2.145 (17)	Mn(5)–O(25)	1.822 (15)
Mn(2)–O(50)	1.872 (14)	Mn(5)–O(61)	1.890 (15)
Mn(2)–N(26)	2.151 (17)	Mn(5)–O(63)	2.136 (16)
		Mn(5)–O(72)	2.152 (16)
Mn(3)–O(7)	2.339 (14)	Mn(5)–N(80)	2.190 (20)
Mn(3)–O(33)	1.932 (15)		
Mn(3)–O(50)	1.896 (14)	Mn(1)···Mn(2)	3.876 (6)
Mn(3)–O(51)	2.200 (14)	Mn(1)···Mn(3)	3.866 (6)
Mn(3)–O(61)	1.878 (15)	Mn(1)···Mn(4)	3.814 (6)
Mn(3)–O(62)	1.907 (15)	Mn(1)···Mn(5)	3.983 (6)
Mn(3)···Mn(4)	2.817 (6)	Mn(3)···Mn(5)	3.408 (6)
Mn(2)···Mn(3)	3.406 (6)	Mn(4)···Mn(5)	3.425 (6)
Mn(2)···Mn(4)	3.443 (6)	Mn(2)···Mn(5)	5.914 (6)
	Angles		
O(6)–Mn(1)–O(6)′	112.0 (8)	O(7)–Mn(1)–O(16)	113.9 (5)
O(6)–Mn(1)–O(7)	56.1 (5)	O(7)–Mn(1)–O(17)	76.2 (5)
O(6)–Mn(1)–O(16)	82.9 (5)	O(16)–Mn(1)–O(16)′	88.3 (7)
O(6)–Mn(1)–O(17)	139.6 (5)	O(16)–Mn(1)–O(17)	77.1 (5)
O(7)–Mn(1)–O(7)′	99.5 (7)	O(17)–Mn(1)–O(17)′	114.1 (7)
O(6)–Mn(2)–O(15)	91.3 (6)	O(15)–Mn(2)–N(26)	89.2 (7)
O(6)–Mn(2)–O(32)	89.1 (6)	O(32)–Mn(2)–O(41)	175.0 (6)
O(6)–Mn(2)–O(41)	94.7 (6)	O(32)–Mn(2)–O(50)	93.5 (6)
O(6)–Mn(2)–O(50)	88.3 (6)	O(32)–Mn(2)–N(26)	88.3 (6)
O(6)–Mn(2)–N(26)	177.4 (7)	O(41)–Mn(2)–O(50)	89.9 (6)
O(15)–Mn(2)–O(32)	86.2 (6)	O(41)–Mn(2)–N(26)	87.9 (6)
O(15)–Mn(2)–O(41)	90.4 (7)	O(50)–Mn(2)–N(26)	91.2 (6)
O(15)–Mn(2)–O(50)	179.5 (7)		
O(7)–Mn(3)–O(33)	88.3 (5)	O(33)–Mn(3)–O(62)	84.6 (6)
O(7)–Mn(3)–O(50)	91.8 (5)	O(50)–Mn(3)–O(51)	93.1 (6)
O(7)–Mn(3)–O(51)	174.8 (5)	O(50)–Mn(3)–O(61)	81.3 (6)
O(7)–Mn(3)–O(61)	92.7 (6)	O(50)–Mn(3)–O(62)	176.5 (6)
O(7)–Mn(3)–O(62)	90.6 (5)	O(51)–Mn(3)–O(61)	90.0 (6)
O(33)–Mn(3)–O(50)	98.0 (6)	O(51)–Mn(3)–O(62)	84.6 (6)
O(33)–Mn(3)–O(51)	89.1 (6)	O(61)–Mn(3)–O(62)	96.0 (6)
O(33)–Mn(3)–O(61)	178.8 (6)		
O(16)–Mn(4)–O(42)	86.6 (6)	O(42)–Mn(4)–O(71)	84.8 (7)
O(16)–Mn(4)–O(50)	92.4 (5)	O(50)–Mn(4)–O(52)	93.8 (6)
O(16)–Mn(4)–O(52)	172.3 (6)	O(50)–Mn(4)–O(61)	81.4 (6)
O(16)–Mn(4)–O(61)	95.0 (6)	O(50)–Mn(4)–O(71)	177.5 (7)
O(16)–Mn(4)–O(71)	87.6 (6)	O(52)–Mn(4)–O(61)	90.5 (6)
O(42)–Mn(4)–O(50)	97.7 (6)	O(52)–Mn(4)–O(71)	86.5 (6)
O(42)–Mn(4)–O(52)	88.0 (6)	O(61)–Mn(4)–O(71)	96.0 (6)
O(42)–Mn(4)–O(61)	178.2 (6)		
O(17)–Mn(5)–O(25)	88.3 (6)	O(25)–Mn(5)–N(80)	88.8 (7)
O(17)–Mn(5)–O(61)	88.6 (6)	O(61)–Mn(5)–O(63)	91.5 (6)
O(17)–Mn(5)–O(63)	99.6 (6)	O(61)–Mn(5)–O(72)	91.8 (6)
O(17)–Mn(5)–O(72)	91.6 (6)	O(61)–Mn(5)–N(80)	94.4 (7)
O(17)–Mn(5)–N(80)	175.9 (7)	O(63)–Mn(5)–O(72)	168.4 (6)
O(25)–Mn(5)–O(61)	176.8 (7)	O(63)–Mn(5)–N(80)	83.2 (7)
O(25)–Mn(5)–O(63)	88.1 (6)	O(72)–Mn(5)–N(80)	85.5 (7)
O(25)–Mn(5)–O(72)	89.2 (6)		

where metal–metal bonding to assist aggregation would obviously not be present. Other examples in Mn chemistry include $Mn_6O_2(piv)_{10}(pivH)_4$ where pivH is pivalic acid[27] and $Mn_{12}O_{12}(O_2CR)_{16}(H_2O)_4$ (R = Me,[28] Ph[29]). In iron chemistry, octanuclear $[Fe_8O_2(OH)_{12}(TACN)_6]Br_8$ (TACN = 1,4,7-triazacyclononane)[13] and undecanuclear[17] $[Fe_{11}O_6(OH)_6(O_2CPh)_{15}]$ have both been structurally characterized; these complexes were obtained by hydrolysis reactions of small-nuclearity starting materials and are held together by oxide and hydroxide bridges.

Table IV. Molar Magnetic Susceptibility (χ_M) and Effective Magnetic Moment per Molecule (μ_{eff}/Molecule) for $[Mn_9O_4(O_2CPh)_8(sal)_4(salH)_2(pyr)_4]$

	χ_M, cgsu		μ_{eff}/molecule, μ_B	
T, K	exptl	calcd[a]	exptl	calcd[a]
300.91	0.05808	0.05868	11.82	11.88
280.79	0.06098	0.06146	11.70	11.75
260.66	0.06446	0.06458	11.59	11.60
239.89	0.06808	0.06826	11.43	11.44
220.39	0.07215	0.07224	11.28	11.28
200.26	0.07714	0.07704	11.12	11.11
180.01	0.08299	0.08284	10.93	10.92
160.02	0.09015	0.08984	10.74	10.72
140.00	0.09917	0.09870	10.54	10.51
119.26	0.1113	0.1108	10.30	10.28
100.24	0.1267	0.1259	10.08	10.05
88.86	0.1387	0.1378	9.93	9.90
79.36	0.1508	0.1500	9.78	9.76
70.00	0.1653	0.1650	9.62	9.61
59.98	0.1874	0.1854	9.48	9.43
50.01	0.2142	0.2123	9.25	9.22
40.00	0.2509	0.2496	8.96	8.93
29.99	0.3034	0.3036	8.53	8.53
20.00	0.3841	0.3878	7.84	7.88
10.00	0.5430	0.5566	6.59	6.67
8.00	0.6139	0.6286	6.27	6.34
6.00	0.7402	0.7446	5.96	5.98
5.00	0.8504	0.8323	5.83	5.77

[a] The parameters resultant from least-squares fitting for the data are the following: $J_1 = -0.97$, $J_2 = -11.2$, $J_3 = -26.2$ cm^{-1}; $g = 2.0$; TIP = 400 × 10^{-6} cgsu; $\chi_{dia} = -12.67 \times 10^{-4}$ cgsu;`MW 2662.45.

Magnetic Susceptibility Study. The results of a variable-temperature magnetic susceptibility study of $Mn_9O_4(O_2CPh)_8(sal)_4(salH)_2(pyr)_4$ (**5**) are presented in Figure 4 and Table IV. The effective magnetic moment, μ_{eff}, per Mn_9 molecule decreases gradually from 11.82 μ_B at 300.9 K to 9.25 μ_B at 50.0 K. Below ~50 K, μ_{eff} per Mn_9 molecule decreases more rapidly with decreasing temperature to a value of 5.83 μ_B at 5.0 K. Since **5** is comprised of an Mn^{II} ion sandwiched by two $Mn^{III}{}_4(\mu_3\text{-}O)_2$ moieties of the same butterfly arrangement as we recently found[9] for $[Mn^{III}{}_4O_2(O_2CMe)_7(bpy)_2](ClO_4)\cdot 3H_2O$ (**3**), it is relevant to make a comparison with the magnetic susceptiblity data for **3**. Compound **3** has a μ_{eff} per Mn_4 molecule that gradually decreases from 7.96 μ_B at 300.6 K to 6.32 μ_B at 40.0 K, whereupon a further decrease in temperature leads to a small increase to 6.82 μ_B at 5.0 K. Per two Mn_4 units of compound **3**, μ_{eff} would vary (multiply values for **3** by $2^{1/2}$) from 11.26 μ_B at 300.6 K to 8.94 μ_B at 40.0 K and then increase to 9.64 μ_B at 5.0 K. Thus, the variation in μ_{eff} per Mn_9 molecule of **5** in the range of 300–50 K is not unlike the variation of $2^{1/2}$ times the μ_{eff} per Mn_4 molecule of **3**. In the absence of appreciable magnetic exchange interactions, the Mn^{II} ion in **5** would be expected to make a relatively temperature-independent contribution to μ_{eff} for the Mn_9 molecule.

A theoretical model to interpret the magnetic susceptibility data for **5** was sought. At the outset it has to be realized that this was a formidable task, for with eight Mn^{III} ($S = 2$) ions and one Mn^{II} ($S = {}^5/_2$) ion there is a total degeneracy of $(2S_{Mn^{III}} + 1)^8(2S_{Mn^{II}} + 1) = 2\,343\,750$. It is simple to realize that, as a result of magnetic exchange interactions, the nonanuclear complex **5** has electronic states with total spin values in the range ${}^{37}/_2$, ${}^{35}/_2$, ${}^{33}/_2$, ..., ${}^3/_2$, ${}^1/_2$. However, it took an appreciable amount of time with a computer program employing the mathematical model given below to identify all of the 209 725 different electronic states for **5**.

The general spin Hamiltonian characterizing the pairwise isotropic magnetic exchange interaction in a polynuclear complex is given by eq 1. We assumed that there is no exchange between

$$\hat{H} = -2\sum_{i,j}^{i\neq j} J_{ij}\hat{S}_i\cdot\hat{S}_j \qquad (1)$$

two metals that are each located in a different butterfly unit. Each

---

(27) Baikie, A. R. E.; Howes, A. J.; Hursthouse, M. B.; Quick, A. B.; Thornton, P. *J. Chem. Soc., Chem. Commun.* **1986**, 1587.

(28) Lis, T. *Acta Crystallogr., Sect. B: Struct. Crystallogr. Cryst. Chem.* **1980**, *B36*, 2042.

(29) Vincent, J. B.; Folting, K.; Streib, W. E.; Huffman, J. C.; Chang, H.-R.; Hendrickson, D. N.; Christou, G., submitted for publication.

Table V. Distribution of Energy States for Mn_9 Complex **5**

energy, cm^{-1}	no. of states	energy, cm^{-1}	no. of states
$E > 2000$	0	$500 > E > 0$	92409
$2000 > E > 1500$	1042	$0 > E > -100$	3077
$1500 > E > 1000$	21757	$-100 > E > -200$	145
$1000 > E > 500$	91295	total	209 725

of the nine manganese ions of **5** are assigned spin operators according to

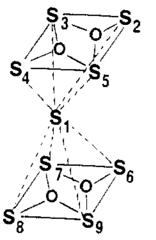

With the one above assumption, the spin Hamiltonian in eq 1 becomes that shown in eq 2. Because the $\hat{S}_3$ and $\hat{S}_5$ Mn^{III} ions are the central dioxide-bridged ions in one butterfly ($\hat{S}_7$ and $\hat{S}_9$ Mn^{III} ions in the other) and there is a C_2 axis at the Mn^{II} ion, $J_3 = J_{35} = J_{79}$ and one parameter (J_2) characterizes all of the interactions in eq 3. Furthermore, it is assumed in eq 2 that $J_{24} = J_{68} = 0$, for the two Mn^{III} ions at the wing tips of each butterfly are far apart. This second assumption is substantiated by noting that when the susceptibility data for the butterfly $Mn_4(\mu_3\text{-}O)_2$ complex **3** were fit, it was found[9] that the analogous J value was zero.

$$\hat{H} = -2(\sum_{j=2}^{9} J_{1j}\hat{S}_1\cdot\hat{S}_j) - 2(J_{23}\hat{S}_2\cdot\hat{S}_3 + J_{34}\hat{S}_3\cdot\hat{S}_4 + J_{45}\hat{S}_4\cdot\hat{S}_5 + J_{52}\hat{S}_5\cdot\hat{S}_2 + J_{35}\hat{S}_3\cdot\hat{S}_5 + J_{24}\hat{S}_2\cdot\hat{S}_4) - 2(J_{67}\hat{S}_6\cdot\hat{S}_7 + J_{78}\hat{S}_7\cdot\hat{S}_8 + J_{89}\hat{S}_8\cdot\hat{S}_9 + J_{96}\hat{S}_9\cdot\hat{S}_6 + J_{68}\hat{S}_6\cdot\hat{S}_8 + J_{79}\hat{S}_7\cdot\hat{S}_9) \quad (2)$$

$$J_2 \equiv J_{23} = J_{34} = J_{45} = J_{52} = J_{67} = J_{78} = J_{89} = J_{96} \quad (3)$$

As a third reasonable assumption we took all of the pairwise interactions between the Mn^{II} ion and any one of the eight Mn^{III} ions as being equal and gauged by the parameter J_1. This gives the spin Hamiltonian in eq 4. In order to determine the eigenvalues of the spin Hamiltonian in eq 4 without determining the eigenvectors (products of spin functions), the vector coupling method of Kambe[30,31] was employed. A vector coupling scheme is identified so that $\hat{S}_i\cdot\hat{S}_j$ operators in eq 4 can be replaced by $\hat{S}_i^2$ operators, the eigenvalues of which can be evaluated simply as $\hat{S}_i^2\psi = S_i(S_i + 1)\psi$, where, for example, $S_i = 2$ for an Mn^{III} ion and $\hat{S}_i^2\psi = 2(3)\psi = 6\psi$. An appropriate vector coupling scheme for complex **5** is shown in eq 5.

$$\hat{H} = -2J_1(\hat{S}_1\cdot\hat{S}_2 + \hat{S}_1\cdot\hat{S}_3 + \hat{S}_1\cdot\hat{S}_4 + \hat{S}_1\cdot\hat{S}_5 + \hat{S}_1\cdot\hat{S}_6 + \hat{S}_1\cdot\hat{S}_7 + \hat{S}_1\cdot\hat{S}_8 + \hat{S}_1\cdot\hat{S}_9) - 2J_2(\hat{S}_2\cdot\hat{S}_3 + \hat{S}_3\cdot\hat{S}_4 + \hat{S}_4\cdot\hat{S}_5 + \hat{S}_5\cdot\hat{S}_2 + \hat{S}_6\cdot\hat{S}_7 + \hat{S}_7\cdot\hat{S}_8 + \hat{S}_8\cdot\hat{S}_9 + \hat{S}_9\cdot\hat{S}_6) - 2J_3(\hat{S}_3\cdot\hat{S}_5 + \hat{S}_7\cdot\hat{S}_9) \quad (4)$$

$$\begin{aligned}
\hat{S}_A &= \hat{S}_2 + \hat{S}_4 \\
\hat{S}_B &= \hat{S}_3 + \hat{S}_5 \\
\hat{S}_C &= \hat{S}_6 + \hat{S}_8 \\
\hat{S}_D &= \hat{S}_7 + \hat{S}_9 \\
\hat{S}_E &= \hat{S}_A + \hat{S}_B \\
\hat{S}_F &= \hat{S}_C + \hat{S}_D \\
\hat{S}_G &= \hat{S}_E + \hat{S}_F \\
\hat{S}_T &= \hat{S}_G + \hat{S}_1
\end{aligned} \quad (5)$$

With the above vector coupling scheme the various $\hat{S}_i\cdot\hat{S}_j$ operators in eq 4 can be represented in terms of $\hat{S}_i^2$ and $\hat{S}_j^2$ operators as indicated by eq 6. The relationships given in eq 6 can be used to rewrite the spin Hamiltonian eq 4 as shown in eq 7. Since $S_1 = {}^5/_2$ and all of the eigenvalues $S_2 = S_3 = S_4 = S_5 = S_6 = S_7 = S_8 = S_9 = 2$, the spin Hamiltonian can be further simplified to eq 8. The allowed values of the eigenvalues of S_A, S_B, S_C, S_D, S_E, S_F, S_G, and S_T are obtained from the addition rule for multiple spin vectors, where, for example, S_A takes the values of $S_2 + S_4$, $S_2 + S_4 - 1$, ..., $|S_2 - S_4|$. The energy of each state is determined by the set of S_A, S_B, ..., S_T values and is given by eq 9. In eq 9 the constant term (${}^{35}/_4 J_1 + 24J_3$) has been dropped because it contributes equally to all states.

$$\begin{aligned}
\hat{S}_A\cdot\hat{S}_A - \hat{S}_2\cdot\hat{S}_2 - \hat{S}_4\cdot\hat{S}_4 &= 2\hat{S}_2\cdot\hat{S}_4 \\
\hat{S}_B\cdot\hat{S}_B - \hat{S}_3\cdot\hat{S}_3 - \hat{S}_5\cdot\hat{S}_5 &= 2\hat{S}_3\cdot\hat{S}_5 \\
\hat{S}_C\cdot\hat{S}_C - \hat{S}_6\cdot\hat{S}_6 - \hat{S}_8\cdot\hat{S}_8 &= 2\hat{S}_6\cdot\hat{S}_8 \\
\hat{S}_D\cdot\hat{S}_D - \hat{S}_7\cdot\hat{S}_7 - \hat{S}_9\cdot\hat{S}_9 &= 2\hat{S}_7\cdot\hat{S}_9 \\
\hat{S}_E\cdot\hat{S}_E - \hat{S}_A\cdot\hat{S}_A - \hat{S}_B\cdot\hat{S}_B &= 2\hat{S}_A\cdot\hat{S}_B = 2(\hat{S}_2 + \hat{S}_4)\cdot(\hat{S}_3 + \hat{S}_5) \\
&= 2(\hat{S}_2\cdot\hat{S}_3 + \hat{S}_3\cdot\hat{S}_4 + \hat{S}_4\cdot\hat{S}_5 + \hat{S}_5\cdot\hat{S}_2) \\
\hat{S}_F\cdot\hat{S}_F - \hat{S}_C\cdot\hat{S}_C - \hat{S}_D\cdot\hat{S}_D &= 2\hat{S}_C\cdot\hat{S}_D = 2(\hat{S}_6 + \hat{S}_8)\cdot(\hat{S}_7 + \hat{S}_9) \\
&= 2(\hat{S}_6\cdot\hat{S}_7 + \hat{S}_7\cdot\hat{S}_8 + \hat{S}_8\cdot\hat{S}_9 + \hat{S}_9\cdot\hat{S}_6) \\
\hat{S}_G\cdot\hat{S}_G - \hat{S}_E\cdot\hat{S}_E - \hat{S}_F\cdot\hat{S}_F &= 2\hat{S}_E\cdot\hat{S}_F \\
\hat{S}_T\cdot\hat{S}_T - \hat{S}_G\cdot\hat{S}_G - \hat{S}_1\cdot\hat{S}_1 &= 2\hat{S}_1\cdot\hat{S}_G \\
&= 2(\hat{S}_1\cdot\hat{S}_2 + \hat{S}_1\cdot\hat{S}_3 + \hat{S}_1\cdot\hat{S}_4 + \hat{S}_1\cdot\hat{S}_5 + \hat{S}_1\cdot\hat{S}_6 + \hat{S}_1\cdot\hat{S}_7 + \hat{S}_1\cdot\hat{S}_8 + \hat{S}_1\cdot\hat{S}_9)
\end{aligned} \quad (6)$$

$$\hat{H} = -J_1(\hat{S}_T\cdot\hat{S}_T - \hat{S}_G\cdot\hat{S}_G - \hat{S}_1\cdot\hat{S}_1) - J_2(\hat{S}_E\cdot\hat{S}_E - \hat{S}_A\cdot\hat{S}_A - \hat{S}_B\cdot\hat{S}_B + \hat{S}_F\cdot\hat{S}_F - \hat{S}_C\cdot\hat{S}_C - \hat{S}_D\cdot\hat{S}_D) - J_3(\hat{S}_B\cdot\hat{S}_B - \hat{S}_3\cdot\hat{S}_3 - \hat{S}_5\cdot\hat{S}_5 + \hat{S}_D\cdot\hat{S}_D - \hat{S}_7\cdot\hat{S}_7 - \hat{S}_9\cdot\hat{S}_9) \quad (7)$$

$$\hat{H} = -J_1(\hat{S}_T\cdot\hat{S}_T - \hat{S}_G\cdot\hat{S}_G - {}^{35}\!/_4) - J_2(\hat{S}_E\cdot\hat{S}_E - \hat{S}_A\cdot\hat{S}_A - \hat{S}_B\cdot\hat{S}_B + \hat{S}_F\cdot\hat{S}_F - \hat{S}_C\cdot\hat{S}_C - \hat{S}_D\cdot\hat{S}_D) - J_3(\hat{S}_B\cdot\hat{S}_B + \hat{S}_D\cdot\hat{S}_D - 24) \quad (8)$$

$$E = -J_1[S_T(S_T + 1) - S_G(S_G + 1)] - J_2[S_E(S_E + 1) + S_F(S_F + 1) - S_A(S_A + 1) - S_B(S_B + 1) - S_C(S_C + 1) - S_D(S_D + 1)] - J_3[S_B(S_B + 1) + S_D(S_D + 1)] \quad (9)$$

An iterative least-squares fitting computer program was written to fit the experimental data to a theoretical expression for the molar paramagnetic susceptibility, χ_M, of the Mn_9 complex **5**. This theoretical expression was determined by means of the Van Vleck equation (eq 10).[32] The summations in eq 10 run over all spin states of the complex, where each state is characterized by a total spin S_T and energy E_n. An average g value is assumed to be applicable.

$$\chi_M = \frac{Ng^2\beta^2}{3kT}\,\frac{\sum_n S_T(S_T + 1)(2S_T + 1)\exp(-E_n/kT)}{\sum_n (2S_T + 1)\exp(-E_n/kT)} \quad (10)$$

Before the least-squares fitting computer program was used to fit the susceptibility data for complex **5**, it was tested under several limiting conditions. With $J_1 = J_2 = J_3 = 0$ and $g = 2$ (TIP = 0, also), μ_{eff} per Mn_9 complex was calculated to be 15.0665 μ_B, which agrees with the spin-only μ_{eff} calculated for a noninteracting assembly of eight Mn^{III} ($S = 2$) and one Mn^{II} ($S = {}^5/_2$) as $\mu_{eff} = [4\sum_i S_i(S_i + 1)]^{1/2} = [4\cdot8\cdot6 + 4\cdot{}^5/_2\cdot{}^7/_2]^{1/2} = 15.0665\ \mu_B$. When the parameters were set as $J_3 = -5000\ cm^{-1}$ and $J_1 = J_2 = 0$, the program gave $\mu_{eff}/Mn_9 = 11.446\ \mu_B$ at 300 K, which is what is

---

[30] Kambe, K. *J. Phys. Soc. Jpn.* **1950**, *5*, 48.

[31] Hatfield, W. E. In *Theory and Applications of Molecular Paramagnetism*; Boudreaux, E. A., Mulay, L. N., Eds.; Wiley-Interscience: New York, 1976; Chapter 7.

[32] Van Vleck, J. H. *The Theory of Electric and Magnetic Susceptibilities*; Oxford University: London, 1932.

Table VI. Lowest Energy States for Mn_9 Complex **5**[a]

no.	S_A	S_B	S_C	S_D	S_E	S_F	S_G	S_T	energy, cm^{-1}
1	4	2	4	2	2	2	4	1.5	−151.1625
2	4	1	4	2	3	2	5	2.5	−148.3125
3	4	2	4	1	2	3	5	2.5	−148.3125
4	4	2	4	2	2	2	4	2.5	−146.3125
5	4	2	4	2	2	2	3	0.5	−146.3125
6	4	1	4	1	3	3	6	3.5	−145.4625
7	4	2	4	1	2	3	4	1.5	−143.4625
8	4	1	4	2	3	2	4	1.5	−143.4625
9	4	2	4	2	2	2	3	1.5	−143.4025
10	4	1	4	2	3	2	5	3.5	−141.5225
11	4	2	4	1	2	3	5	3.5	−141.5225
12	4	1	4	1	3	3	5	2.5	−140.6125
13	4	2	4	2	2	2	2	0.5	−140.4925
14	4	2	4	2	2	2	4	3.5	−139.5225
15	4	2	4	1	2	3	4	2.5	−138.6125
16	4	2	4	1	2	3	3	0.5	−138.6125
17	4	1	4	2	3	2	4	2.5	−138.6125
18	4	1	4	2	3	2	3	0.5	−138.6125
19	4	2	4	2	2	2	3	2.5	−138.5525
20	4	2	4	2	2	2	2	1.5	−137.5825
21	4	1	4	1	3	3	6	4.5	−136.7325

[a] See the text for a definition of S_A, S_B, S_C, S_D, S_E, S_F, S_G, and S_T.

expected if the Mn_3–Mn_5 and Mn_7–Mn_9 couples are spin paired due to a strong antiferromagnetic interaction. When the parameters were set at $J_2 = -5000$ cm^{-1} and $J_1 = J_3 = 0$, the program gave $\mu_{eff}/Mn_9 = 5.916$ μ_B, the value expected for complex **5** when the two Mn_4 butterflies are paired up and only the Mn^{II} ion has unpaired electrons.

In fitting the data for **5**, g (=2.0) and TIP (=400 × 10^{-6} cgsu per complex) were kept constant, and the parameters J_1, J_2, and J_3 were varied to fit the data. As can be seen by the solid lines in Figure 4, a very good fit was obtained with $J_1 = -0.97$ (10) cm^{-1}, $J_2 = -11.2$ (1) cm^{-1}, and $J_3 = -26.2$ (1) cm^{-1}. This fit took more than 500 cycles of iteration when the simplex fitting procedure was employed;[33] each cycle required ~15 min CPU time on a VAX 11/780 computer. Calculated and experimental values of χ_M and μ_{eff} are given in Table IV. The distribution of states obtained with the above values of J_1, J_2, and J_3 is given in Table V. The ground state is a quartet $S = {}^3/_2$ state with an energy of −151.16 cm^{-1}. Within 150 cm^{-1} of this ground state there are over 3000 electronic excited states. All 209 725 states of this Mn_9 complex are found within 2000 cm^{-1} of the ground state. In Table VI are given the values of S_A, S_B, ..., S_G, S_T and energies that characterize the ground state and the 20 lowest energy excited states. Obviously there is an appreciable density of states, and several states are thermally populated even at 4 K. According to a Boltzmann distribution, ~32% of the complexes are in the ground state ($S_T = {}^3/_2$) at 4 K, and ~17% are in each of first two excited states ($S_T = {}^5/_2$). This explains why the EPR spectrum for **5** is not revealing even when run at liquid helium temperatures. The X-band EPR spectrum for a polycrystalline sample of **5** at 4 K exhibits a derivative signal at $g = 2.0$ and a very broad feature with a maximum at $g \simeq 4$. When the sample temperature is increased, only the $g = 2.0$ signal can be seen.

The values of the J_1, J_2, and J_3 parameters obtained by fitting the susceptibility data for the Mn_9 complex seem to be quite reasonable. The very weak antiferromagnetic interaction ($J_1 = -0.97$ cm^{-1}) between the central Mn^{II} ion and any one of the eight Mn^{III} ions is reasonable in view of the fact that the $Mn^{II}\cdots Mn^{III}$ distances (3.81–3.98 Å) are appreciably longer than the two different $Mn^{III}\cdots Mn^{III}$ distances (3.41–3.44 and 2.82 Å), which determine the J_2 and J_3 parameters. In addition, with all other factors being equal, an $Mn^{II}\cdots Mn^{III}$ exchange interaction could be weaker than an $Mn^{III}\cdots Mn^{III}$ interaction, because in the former case the d orbitals on the two metal ions are more energetically inequivalent. In fact, in the case of four different structurally characterized $Mn^{II}Mn^{III}$ complexes, we have found[34,35] that J varies from −6 to +1 cm^{-1}.

Finally, the J_2 (=−11.2 cm^{-1}) and J_3 (=−26.2 cm^{-1}) parameters, which gauge the antiferromagnetic exchange interactions in the two Mn_4 butterflies of the Mn_9 complex, compare favorably with those we found[9] for the butterfly complex $[Mn_4O_2(O_2CMe)_7(bpy)_2]ClO_4 \cdot 3H_2O$ (**3**). For this latter complex we found $J_2 = -7.8$ cm^{-1} and $J_3 = -23.5$ cm^{-1}, parameters that are quite close in magnitude to those evaluated for the Mn_4 complex. This is satisfying in the sense that the Mn_4 moieties of the Mn_9 complex **5** are structurally very similar to the Mn_4 butterfly complex **3**.

Concluding Comments

The preparation and X-ray structure of an interesting nonanuclear complex, $[Mn_9O_4(O_2CPh)_8(sal)_4(salH)_2(pyr)_4]$ (**5**), have been reported. There is a central Mn^{II} ion surrounded by two butterfly-like $Mn^{III}{}_4(\mu_2\text{-}O)_2$ units. A detailed theoretical model has been derived by the Kambe vector coupling model to interpret magnetic susceptibility data measured for **5** in the range of 5.0–300.9 K. A good least-squares fit of the data to the theoretical equations was obtained, where the magnetic exchange parameters have been shown to be reasonable by comparison to exchange parameters obtained for an analogous manganese complex.

Each $[Mn_9O_4(O_2CPh)_8(sal)_4(salH)_2(pyr)_4]$ complex in a crystal of **5** can be likened to a single-domain particle of a magnetic metal oxide. Each Mn_9 complex has a high density of states that are thermally populated, for there are 209 725 spin states of **5** that are within 2000 cm^{-1} of the $S = {}^3/_2$ ground state. It remains to be determined whether this Mn_9 complex is a simple paramagnet or whether it exhibits a cooperativity resulting from the pairwise magnetic exchange interaction present in **5**. Studies of the magnetization versus magnetic field need to be carried out at various temperatures to examine this question, as was done by Gorun et al.[17] in their recent study of a $Fe^{III}{}_{11}$ complex. They found that magnetic fields as large as 230 kOe were required to reach a saturation field for their $Fe^{III}{}_{11}$ complex at 1.3 K. From the results of magnetization studies, Gorun et al.[17] concluded that the $Fe^{III}{}_{11}$ complex is not behaving as a simple paramagnet. For example, they found that plots of magnetization as a function of H/T at 2 and 5 K were not congruent. Examination of Table VI shows that the Mn_9 complex **5** has five spin states within ~6 cm^{-1} of the $S = {}^3/_2$ ground state. In fact, if the present theoretical

---

[33] Chandler, J. P. *QCPE* **1973**, *66*.

[34] Schake, A.; Vincent, J. B.; Huffman, J. C.; Christou, G.; Chang, H.-R.; Li, Q.; Hendrickson, D. N., submitted for publication.

[35] Diril, H.; Chang, H.-R.; Zhang, X.; Larsen, S. K.; Potenza, J. A.; Pierpont, C. G.; Schugar, H. J.; Isied, S. S.; Hendrickson, D. N. *J. Am. Chem. Soc.* **1987**, *109*, 6207–6208.

modeling is accurate, the first excited state, which has $S = {}^5/_2$, is only 2.85 cm^{-1} above the ground state. Magnetic fields as large as 230 kOe would lead to such an appreciable Zeeman splitting of the $S = {}^5/_2$ excited spin state that a component of this state becomes the ground state at high magnetic fields. In fact, magnetic anisotropy would lead to magnetic field mixing of the various spin states of **5**. Detailed magnetization studies of **5** are needed; however, it will also be necessary to characterize the relaxation time of the magnetization of **5** to decide whether the Mn_9 complexes in a crystal of **5** are behaving as a simple paramagnet or are exhibiting superparamagnetism or, for that matter, superantiferromagnetism.[36]

Acknowledgment. Funding from National Science Foundation Grant CHE-8507748 (G.C.) and partial funding from National Institutes of Health Grant HL13652 (D.N.H.) are gratefully acknowledged.

Registry No. **5**, 112068-77-6; $Mn_3O(O_2CPh)_6(pyr)_2(H_2O)$, 109862-72-8.

Supplementary Material Available: Tables of anisotropic thermal parameters of manganese ions and all bond lengths and angles for complex **5** (7 pages); listing of calculated and observed structure factors (9 pages). Ordering information is given on any current masthead page. A complete MSC structure report (86109) is available on request from the Indiana University Chemistry library.

---

(36) Néel, L. *C. R. Hebd. Seances Acad. Sci.* **1961**, *252*, 4075–4080; *253*, 9–12; *253*, 203–208.

Thermal Decarbonylation of Molybdenum(II) Carbonyl–Iodide Complexes. Molecular and Electronic Structures of the Mixed-Valence Trinuclear Clusters $Mo_3HI_7L_3$ (L = Tetrahydrofuran, Acetonitrile, Benzonitrile) and Molecular Structures of $MoI_3(EtCN)_3$ and $Mo_2I_4(PhCN)_4$

F. Albert Cotton* and Rinaldo Poli*†

Contribution from the Department of Chemistry and Laboratory for Molecular Structure and Bonding, Texas A&M University, College Station, Texas 77843. Received July 30, 1987

Abstract: Trinuclear cluster compounds of the type $Mo_3HI_7L_3$ (L = THF, CH_3CN, C_6H_5CN) can be obtained by decarbonylation of carbonyl–iodide complexes of molybdenum(II) in the presence of hard-donor ligands. In tetrahydrofuran (THF) an oligonuclear compound of stoichiometry $\{MoI_2(THF)_n\}_x$ (**1**) is formed as the main product. The trinuclear cluster $Mo_3HI_7(THF)_3{\cdot}THF$ (**2**) is obtained from the same reaction in low yields. When MeCN and EtCN are used as solvents, solutions containing the quadruply bonded dimers $Mo_2I_4(RCN)_4$ are obtained, together with other minor insoluble products. Interaction of compound **1** with RCN also gives $Mo_2I_4(RCN)_4$, which is unstable toward loss of the nitrile and cannot be isolated for R = Me and Et. A ligand-exchange reaction with PhCN affords $Mo_2I_4(PhCN)_4$ (**6**), which is stable in the solid state. Other compounds that are produced in smaller yields in these reactions have been isolated and characterized, namely $Mo_3HI_7(MeCN)_3{\cdot}MeCN$ (**3**), $MoI_3(EtCN)_3$ (**4**), and $Mo_3HI_7(PhCN)_3{\cdot}C_6H_5CH_3$ (**5**). Compound **1** also reacts with PMe_3 to afford $Mo_2I_4(PMe_3)_4$ and with I^- to produce the $[Mo_4I_{11}]^-$ anion. A different form of the trinuclear cluster with coordinated THF has also been obtained, $Mo_3HI_7(THF)_3$ (**7**). Crystal data are the following. Compound **2**: orthorhombic; space group *Pcam*; $a = 21.216$ (3), $b = 8.459$ (1), $c = 18.477$ (2) Å; $V = 3316$ (1) Å^3; $Z = 4$; $d_{calcd} = 2.933$ $g{\cdot}cm^{-3}$; $R = 0.0461$, $R_w = 0.0743$ for 148 parameters and 1716 observed data $[F_o^2 > 3\sigma(F_o^2)]$. Compound **3**: orthorhombic; space group *Pcmb*; $a = 7.703$ (1), $b = 17.903$ (2), $c = 20.179$ (2) Å; $V = 2783$ (1) Å^3; $Z = 4$; $d_{calcd} = 3.199$ $g{\cdot}cm^{-3}$; $R = 0.0355$, $R_w = 0.0478$ for 103 parameters and 1661 observations with $F_o^2 > 3\sigma(F_o^2)$. Compound **4**: monoclinic; space group $P2_1/n$; $a = 11.065$ (5), $b = 13.174$ (3), $c = 12.974$ (5) Å; $\beta = 103.70$ (3)°; $V = 1836$ (2) Å^3; $Z = 4$; $d_{calcd} = 2.321$ $g{\cdot}cm^{-3}$; $R = 0.0570$, $R_w = 0.0680$ for 145 parameters and 1379 observations with $F_o^2 > 3\sigma(F_o^2)$. Compound **5**: monoclinic; space group $P2_1/m$; $a = 8.606$ (3), $b = 18.471$ (10), $c = 12.628$ (6) Å; $\beta = 96.38$ (4)°; $V = 1995$ (3) Å^3; $Z = 2$; $d_{calcd} = 2.626$ $g{\cdot}cm^{-3}$; $R = 0.0495$, $R_w = 0.0728$ for 144 parameters and 1594 observations with $F_o^2 > 3\sigma(F_o^2)$. Compound **6**: orthorhombic; space group *Fddd*; $a = 22.941$ (2), $b = 39.516$ (12), $c = 17.336$ (8) Å; $V = 15715$ (15) Å^3; $Z = 16$; $d_{calcd} = 1.879$ $g{\cdot}cm^{-3}$; $R = 0.0664$, $R_w = 0.0827$ for 92 parameters and 851 observations with $F_o^2 > 3\sigma(F_o^2)$. Compound **7**: trigonal; space group *R3m*; $a = 17.112$ (4), $c = 8.599$ (2) Å; $V = 2180.5$ (14) Å^3; $Z = 3$; $d_{calcd} = 4.158$ $g{\cdot}cm^{-3}$; $R = 0.0428$, $R_w = 0.0583$ for 43 parameters and 321 observations with $F_o^2 > 3\sigma(F_o^2)$. The structure of the $Mo_3HI_7L_3$ (L = THF, MeCN, PhCN) clusters consists of an equilateral-triangular arrangement of the metals with strong metal–metal bonding interactions. The faces of the triangle are capped by an iodide and a hydride ligand, and a bridging iodide ion spans each edge. The structure is completed by three terminal iodide ions and three terminal ligands L. The Mo_3I_7 core of the molecules can be described as what would remain from the Mo_6I_8 cluster core found in α-MoI_2, upon removal of a $(\mu_3\text{-}I)Mo_3$ unit. The presence of H is inferred from the diamagnetism and the presence of an ^1H resonance at −10.31 ppm for compound **5**. A molecular orbital treatment of the trinuclear cluster with the Fenske–Hall method is presented.

Molybdenum and tungsten MX_2 (X = Cl, Br, I) compounds are known to exist as extended layered structures containing $[M_6X_8]^{4+}$ cores linked by additional X^- ions, i.e. $\{[M_6X_8]X_2X_{4/2}\}_\infty$, at least in their crystalline form generally referred to as the α-form. Structurally characterized examples are $MoCl_2$[1] and MoI_2,[2] while W_6Br_{16} has also been shown[3] to contain $[W_6Br_8]^{4+}$ units bridged by $[Br_4]^{2-}$ anions. A water adduct of $MoBr_2$, $Mo_6Br_{12}(H_2O)_2$, has also been structurally characterized,[4] as well as the anions

---

† Present address: Department of Chemistry and Biochemistry, University of Maryland, College Park, MD 20742.

(1) Schäfer, H.; von Schnering, H.-G.; Tillack, J.; Kuhnen, F.; Wöhrle, H.; Baumann, H. *Z. Anorg. Allg. Chem.* **1967**, *353*, 281.

(2) Aliev, Z. G.; Klinkova, L. A.; Dubrovin, I. V.; Atovmyan, L. O.; *Russ. J. Inorg. Chem. Engl. Transl.* **1981**, *26*, 1060.

(3) Siepmann, R.; von Schnering, H.-G. *Z. Anorg. Allg. Chem.* **1968**, *357*, 289.

0002-7863/88/1510-0830$01.50/0 © 1988 American Chemical Society